THE UNIVERSITY OF QUEENSLAND
AUSTRALIA

Uncertainty Modelling with Polynomial Chaos Expansions

Stage 2 Report

Celoxis System ID: 149 297

Report release date: 15 June 2016

Research Team

Professor Stephen Tyson
School of Earth Sciences, University of Queensland
Associate Professor Diane Donovan
School of Mathematics and Physics, University of Queensland
Associate Professor Bevan Thompson
School of Mathematics and Physics, University of Queensland
Dr Brodie Lawson
School of Mathematics and Physics, University of Queensland

Citation

Tyson, S., Donovan, D., Thompson, B., & Lawson, B. (2016). *Uncertainty modelling with polynomial chaos expansions: Stage 2 Report.*
ISBN: 978-1-74272-174-3

Disclosure

The UQ, Centre of Coal Seam Gas is currently funded by the University of Queensland 22% ($5 million) and the Industry members 78% ($17.5 million) over 5 years. An additional $3.0 million is provided by industry members for research infrastructure costs. The industry members are QGC, Santos, Arrow and APLNG. The centre conducts research across Water, Geoscience, Petroleum Engineering and Social Performance themes.

For more information about the Centre's activities and governance see http://www.ccsg.uq.edu.au/

Disclaimer

The information, opinions and views expressed in this report do not necessarily represent those of The University of Queensland, the Centre for Coal Seam Gas or its constituent members or associated companies. Researchers within or working with the Centre for Coal Seam Gas are bound by the same policies and procedures as other researchers within The University of Queensland, which are designed to ensure the integrity of research. You can view these policies at: http://ppl.app.uq.edu.au/content/4.-research-and-research-training

The Australian Code for the Responsible Conduct of Research outlines expectations and responsibilities of researchers to further ensure independent and rigorous investigations.

This report has not yet been independently peer reviewed.

Document Control Sheet

Version #	Reviewed by	Revision Date	Brief description of changes

Executive Summary

Traditionally static models have been used to develop strategies for the quantification of petroleum resources and other engineering processes. The focus has been on developing methods that improve our understanding of the range of possible outcomes and thus inform decision making processes to capitalize on unexpectedly good outcomes and to mitigate the impact of poor results.

The cost and complexity of current processes dictate a need to develop new and robust techniques that quantify the range and the relative impact of uncertainty in parameters and inform on how this uncertainty propagates to model outcomes, especially when input information is limited.

Historically Monte-Carlo simulations—multiple repetitions of the simulation using randomly chosen values for input variables—have been used to model such processes. However, depending on the dimension of the 'sample space', good approximations come at the cost of large numbers of simulations.

Polynomial Chaos Expansions (PCE) provide surrogate models that can significantly reduce the number of simulations required to quantify uncertainty, while still retaining a low degree of error. The surrogate polynomial model takes the form

$$Y \approx \sum_{k=0}^{n} Y_k P_k(\varepsilon_1, \dots, \varepsilon_d)$$

where ε_i represents the d uncertain parameters, Y_k are coefficients and P_k are orthogonal polynomials, with expectation $\langle Y \rangle = Y_0$ and variance $\sigma^2 = \langle Y^2 \rangle - \langle Y \rangle^2 = \sum_{k=1}^{n} {Y_k}^2 \langle (P_k)^2 \rangle$.

In Stage 2 of the current project we have developed high-level code to implement, test and calibrate PCE techniques on 3 distinct test models.

- The modeling of a steady state fluid flow, with two uncertain variables, using both intrusive and non-intrusive PCE.
- The modeling of a commercial black box solver, with four uncertain variables, for the quantification of peak and total gas recovery.
- Modeling of discrete highly non-linear processes using rule based cellular automata.

In each case we have developed and implemented workflows that reflect critical aspects of these scenarios. In particular we have constructed distinct surrogate models of increasing order, thus determining the convergence and error behavior of the solution.

Results show that PCE performs well on these models, and therefore has the potential to value add to industry based research and development.

Table of Contents

Contents

0. Table of Figures

1. Stage 2 Outcomes

We have:

- **i.** Augmented the research team with the right skills to execute an assessment of the feasibility of PCE for commercialization. Contributors to Stage 2 research include D Donovan, B Lawson, M Tas, B Thompson, S Tyson, F Zhou.
- **ii.** Extended and updated the literature review covering a wider class of applications and techniques for numerical integration.
- **iii.** Compared and contrasted non-intrusive and intrusive PCE techniques, concluding that non-intrusive PCE provides greater flexibility particularly when the complexity of the underlying model and the number of uncertain parameters is increased.
- **iv.** Updated and reviewed the documentation on the supporting mathematical theory.
- **v.** Generated the basic code necessary for surface fitting using orthogonal

polynomials.

vi. Generated code for numerical integration using Gaussian quadrature and sparse grid quadrature.

vii. Developed workflows.

viii. Defined calibration and validation procedures.

ix. Implemented workflows and calibration and validation procedures on three distinct prototype models.

x. Prepared 3 articles on the quantification of uncertainty using PCE.

Note 1: Non-intrusive PCE does not require modification of the existing "Model" code. Higher dimensionality may increase the complexity of non-intrusive PCE however methods such as sparse grid quadrature can help alleviate this problem.[1] While intrusive PCE may deliver an elegant one-time solution to a system of equations and the PCE coefficients, the disadvantage is that the code is often application specific, with the reformulation being significantly larger than the original system. This results in increased time horizons for approximating solutions to systems of ODEs, and a process that is infeasible for systems of PDEs.[2]

Note 2: While sparse grid quadrature is complex it has the advantage that data points can be reused as the order is increased. In contrast Gaussian quadrature requires the generation of new points.

2. Workflows

The workflow given below details steps necessary to develop the PCE enabling software. In any implementation of PCE many of the workflow steps will be automated.

W1. Identify relevant "Model" to be approximated by surrogate PCE.

W2. For the "Model" $M(\theta)$ identify uncertain variables θ, their ranges and associated probability distributions.

W3. Rescale the uncertain variables θ to standard ranges, relabeled ε here.

W4. Set the tolerance for error.

W5. Based on the probability distribution identify the correct class of orthogonal polynomials (e.g. Hermite, Legendre …).

W6. For Model $M(\theta)$ determine the method of implementation (i.e. non-intrusive or intrusive)

W7. Set the initial order n of the PCE.

W8. Execute PCE workflow (see below) to obtain a surrogate PCE of the form

[1] B Debusschere, H Najm, K Sargsyan and C Safta, Polynomial Chaos based uncertainty propagation Intrusive and Non-Intrusive Methds, USC UQ Summer School, Sandia National Laboratories, 2013

[2] B Debusschere, H Najm, K Sargsyan and C Safta, Polynomial Chaos based uncertainty propagation Intrusive and Non-Intrusive Methds, USC UQ Summer School, Sandia National Laboratories, 2013

$$Y \approx \sum_{k=0}^{n} Y_k P_k(\varepsilon_1, \cdots, \varepsilon_d)$$

W9. Calibrate and validate the PCE.

W10. From the PCE extract statistical information such as the cumulative distribution function (CDF), expectation and variance (mean and standard deviation) and/or execute parameter finding by recovering the physical values of the underlying uncertain variables.

Specific workflow for non-intrusive PCE, to be inserted in step **W8** above.

NI.1. Based on the number of uncertain variables determine the method of numerical integration; i.e. Gaussian quadrature or sparse grid quadrature.

NI.2. Set the order of the PCE (degree of the polynomial expansion).

NI.3. Generate training (quadrature) points, associated weights and code the numerical integration method.

NI.4. Evaluate the $M(\theta)$ at the training points.

NI.5. Based on training points determine the coefficients

$$Y_{\boldsymbol{k}} = \frac{\int_{\Omega} \mathrm{M}(\boldsymbol{\xi}) P_{\boldsymbol{k}}(\boldsymbol{\xi}) \rho(\boldsymbol{\xi})\, d\boldsymbol{\xi}}{\langle P_{\boldsymbol{k}}(\boldsymbol{\xi})^2 \rangle}$$

NI.6. Output the PCE surrogate model $Y \approx \sum_{k=0}^{n} Y_k P_k(\varepsilon_1, \cdots, \varepsilon_d)$.

Specific workflow for intrusive PCE, to be inserted in step **W8** above.

I.1. Develop a mathematical formulation for $M(\theta)$ based on spectral expansion of orthogonal polynomials.

I.2. Identify and evaluate subsidiary conditions.

I.3. Solve the expanded model, to obtain the coefficients Y_k.

I.4. Output the PCE surrogate model $Y \approx \sum_{k=0}^{n} Y_k P_k(\varepsilon_1, \cdots, \varepsilon_d)$.

3. Model Calibration and Validation Procedures

Calibration: an initial filter for the checking of convergence

C1. For the given order of the PCE determine the coefficients Y_k of the PCE.

C2. Increment the order of the PCE and determine the coefficients Y_k of the new PCE.

C3. If the changes in coefficients are not within the given tolerance return to Step C2.

C4. Otherwise accept the coefficients and the surrogate model.

Validation

V1. Calculate Root Mean Square (RMS) error based on the difference of $M(\theta)$ and $P(\theta)$ at the training point.

V2. If the error is not within the set tolerances return to Workflow **W7** and increase the order of the PCE expansion.

V3. Use coarse Monte Carlo/Latin hypercube sampling to generate an evenly distributed population of test points across the parameter space.

V4. Compute the absolute difference between the Model and the PCE surrogate at these data points.

V5. If the error is not within the set tolerances return to Workflow **W7** and increase the order of the PCE.

V6. Visualize the response surface to check for anomalies.

In Validation Step **V3** latin hypercube sampling is the preferred choice as it ensures good coverage of the parameter space and thus a good representation of the underlying variability of the variables. In latin hypercube sampling, upper and lower bounds on the range of values for each parameter are specified with each range being subdivided into *n* equally-spaced sub-intervals thereby subdividing the parameter space into equally likely hyper-subcubes. A latin hypercube sample is a set of *n* sample points whereby each sample is the only one intersecting the corresponding subdivisions.

It is worth noting that the approximation of error for PCE is a current area of intense research. It is known that any random variable is a function defined on a probability space and can be approximated in mean square by a finite PCE. So we can obtain good approximations to the moments of the random variable including mean and variance of the cumulative distribution function. This does not always translate to arbitrary precision uniformly across the parameter space, although it does for most problems of interest. However, in practice the PCE is seen as a model choice to represent what is known about the random variable. The rule of thumb is that the order of the PCE should be increased until successive results are within a given tolerance. This is not always fail proof but usually a low order PCE generally gives the desired error.[3]

4. Prototype Testing and Results

In the first two prototypes we step through the Workflow.

Model 1. Surrogate to a 2-variable DE model with analytical solution.

W1. The relevant "Model" to be approximated by PCE

Solute transport in groundwater:

Solutes are transported through groundwater primarily via two processes, dispersion and advection. In the 1-dimensional case, possibly corresponding to a 3-dimensional

[3] B Debusschere, H Najm, K Sargsyan and C Safta, Polynomial Chaos based uncertainty propagation Intrusive and Non-Intrusive Methds, USC UQ Summer School, Sandia National Laboratories, 2013

stream-tube with homogeneous properties, the spread of a solute S is modelled by

$$R_f \frac{\partial S}{\partial t} = D_L \frac{\partial^2 S}{\partial x^2} - V_w \frac{\partial S}{\partial x}$$

with R_f the retardation factor, D_L the dispersivity and V_w the velocity of the groundwater, each expressed in terms of specific physical properties of the transport material. This model has an exact solution

$$S(x,t) = \frac{1}{2} S_0 \left[erfc\left(\frac{R_F x - V_w t}{\sqrt{4 D_L R_f t}}\right) + e^{\frac{V_w x}{D_l}} erfc\left(\frac{R_F x + V_w t}{\sqrt{4 D_L R_f t}}\right)\right]..$$

W2. For $S(x,t)$, two uncertain variables, both with uniform distribution and their ranges are

-hydraulic conductivity K (related to permeability), range $[1.0E-7, 1.0E-3]\ cm/s$

-organic carbon partition coefficient K_{oc} , range $[20,500]\ cc/g$

W3. Rescale the parameters to standard ranges.

$$\xi_1 = \frac{2(K-\overline{K})}{K_{max}-K_{min}} \qquad \xi_2 = \frac{2(K_{oc}-\overline{K_{oc}})}{K_{ocmax}-K_{ocmin}}$$

W4. The error tolerance was set at 3×10^{-2}.

W5. The correct class of orthogonal polynomials is Legendre.

$$(m+1)L_{m-1}(\epsilon) = (2m+1)\varepsilon L_m(\varepsilon) - mL_{m-1}(\varepsilon)$$

$$L_1(\varepsilon) = \epsilon$$

$$L_0(\varepsilon) = 1$$

W6. Both intrusive and non-intrusive PCE surrogate models were developed. Only non-intrusive will be reported here.

W7. The initial order *n* of the PCE was set at *n=1*.

W8. Workflow for non-intrusive PCE was executed.

NI.1. Both Gaussian quadrature and sparse grid quadrature were tested, but only Gaussian quadrature is reported on here.

NI.2. Training (quadrature) points, associated weights and numerical integration code were generated. The number of training (quadrature) points are given below

PCE Level	Number of training points
n=1	4
n=2	9
n=5	36
n=10	121

Table 1 Training Points

The training points for *n=5* are displayed in Figure 1.

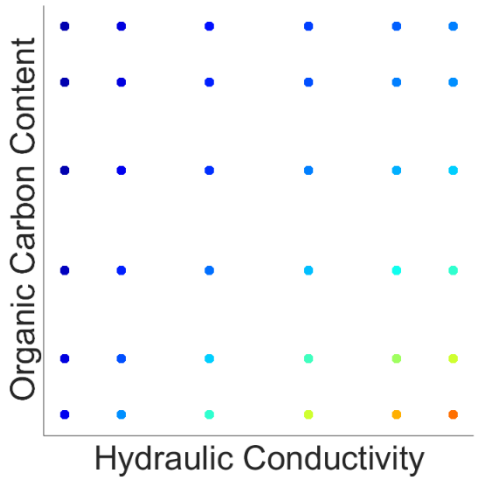

Figure 1: Heat map of training points, showing S(x,t) evaluated at 36 points, chosen to minimise numerical integration error.

NI.3. $S(x,t)$ was evaluated at *t=1000* and the penetration distance was obtained for the appropriate training (quadrature points) (K, K_{oc}). The coefficients Y_k were determined using

$$Y_k = \frac{\int_\Omega \mathrm{M}(\xi) P_k(\xi) \rho(\xi)\, d\xi}{\langle P_k(\xi)^2 \rangle}.$$

NI.4. A PCE surrogate model $Y \approx \sum_{k=0}^{n} Y_k P_k(\varepsilon_1, \cdots, \varepsilon_d)$ was determined.

W9. Execute calibration and validation procedures.

Calibration

C1.—C3. The order was initially set at *n=1* and incremented to *n=2* and *n=3* with the change in the Y_k between orders 2 and 3 converging. Hence level 2 was accepted for coefficient convergence.

C4. The coefficients and the surrogate model were accepted.

Validation

V1.-V6. The point to point Root Mean Square (RMS) error across the entire parameter space was calculated as

$$RMS = \sqrt{\frac{E}{N}}$$

where N is the number of points and

$$E = \sum_{i=1}^{N} \left(S(x_i, t_i) - S_{PCE}(x_i, t_i) \right)^2.$$

The order of the PCE was increased until *n=5* at which point the required tolerances were obtained. As the computation was extremely fast and this was a test case, the order was increased to *n=10*. The following graphics display the point to point error for two specific values of (K, K_{oc}) when *n=10.*

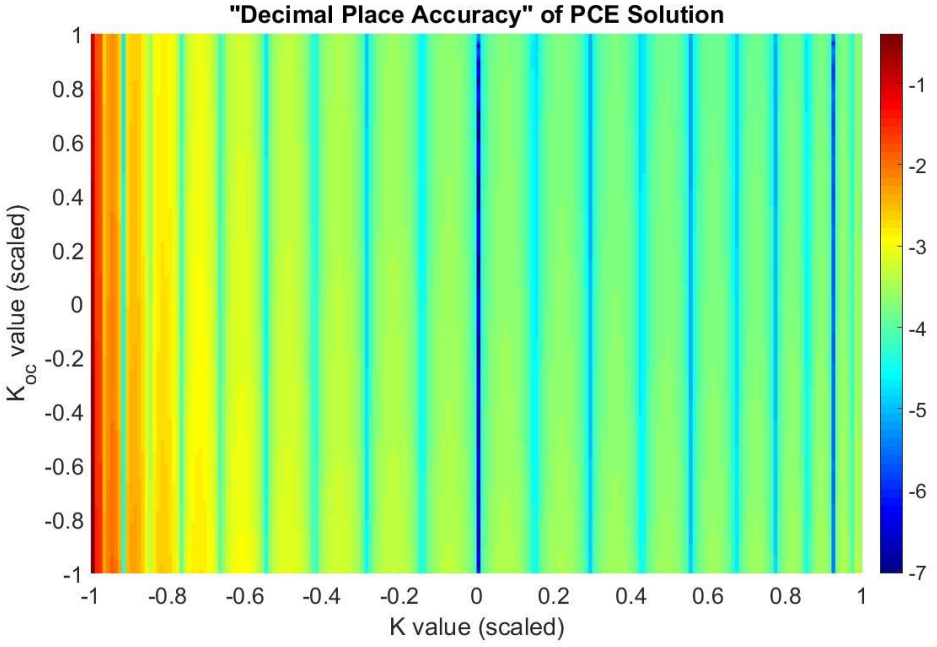

Figure 2 Point to point RMS error across the entire parameter space showing errors of 10^{-1} at extremes and as low as 10^{-7}.

This map indicates that the change in the uncertainty in the value for the organic carbon partition coefficient does not impact on the error estimates. The regions of low error correspond to the values of the training points for the hydraulic conductivity. However, for the regions in between these training points the error is less than 10^{-3} except when the hydraulic conductivity is low there is little penetration and sharp fronts, but even in this case the PCE has maintained an error of less than 10^{-1}.

The following two plots emphasize the error decreases as the order of the PCE increases.

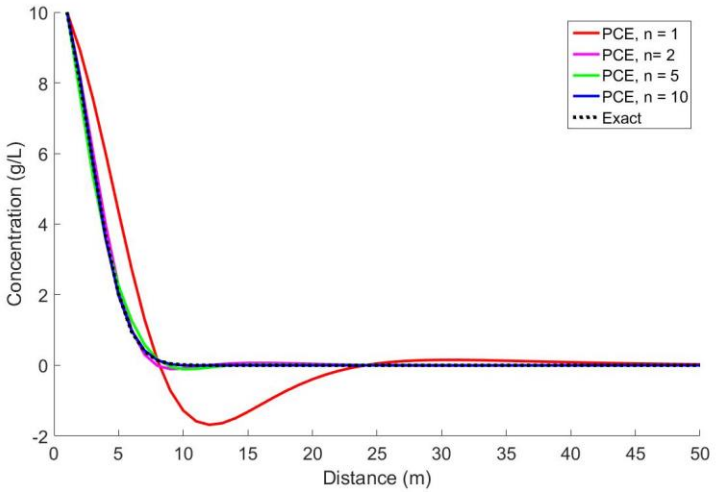

Figure 3. Plot of solute concentration for $(K, K_{oc}) = (-0.81, 0.85)$, at varying penetration distance from source when t=1000 days and for PCE up to order 10. The "Model's" solution S(x,1000) is displayed in black.

In Figure 3 it can be seen that when the PCE order is 1 in a linear approximation to the "Model" the concentration dips below zero. While this is physically infeasible in a theoretical sense it is entirely possible and once again demonstrates the power of higher order PCE over linear systems.

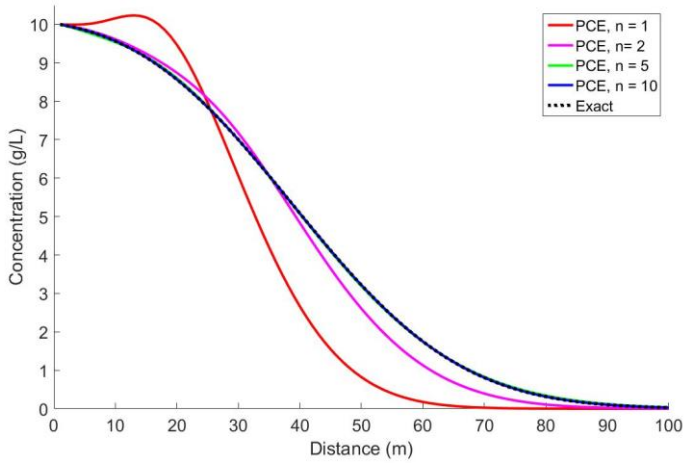

,

Figure 4 Plot of solute concentration for $(K, K_{oc}) = (0.75, -0.9)$ at varying penetration distance from source when t=1000 days and for PCE up to order 10. The "Model's" solution S(x,1000) is displayed in black.

The model was not tested against a Monte Carlo or latin hypercube simulation, but when tested against the exact solution it was found that *n=5* gave results within the given error tolerances.

At this stage the PCE surrogate produced a good approximation within the given tolerances across the full surface, as displayed in Figure 5.

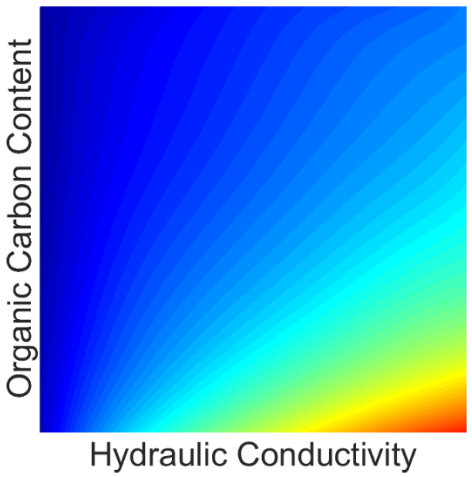

Figure 5 Full surrogate response surface for penetration distance of the solute at t=1000 days as a function of the hydraulic conductivity and the organic carbon partition coefficient.

W9. Statistical information and inverse quantification

The Cumulative Distribution Function (CDF) was calculated to determine confidence intervals for the penetration distance at *t=1000* days. Since an exact solution exists for this problem it was possible to compare the CDF for the PCE surrogate model with the CDF for the exact solution. This information is given in Figure 6. It can be seen that for *n=10* there is almost an exact correspondence.

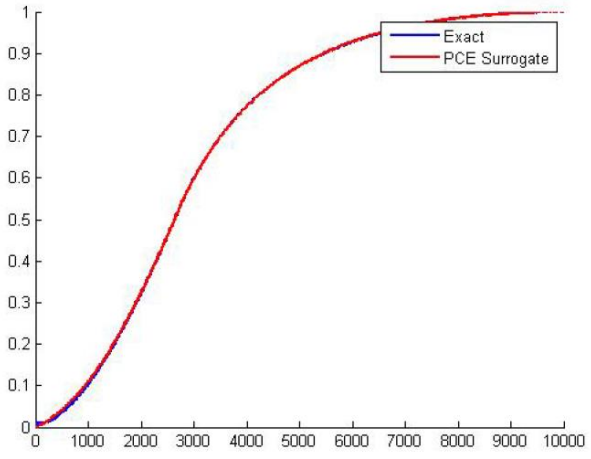

Figure 6 CDF for PCE and exact solution, showing CDF for the penetration distance at t=1000 days.

Parameter Finding and Inverse Uncertainty Quantification

The problem of inverse uncertainty quantification is then to accurately and quickly explore the parameter space in order to find those points or regions with that minimise error.

Artificial data was generated, representative values for the hydraulic conductivity and organic carbon partition coefficient were chosen and used in the "Model" to obtain an output value at this point. For instance, taking $\mathrm{K} = 7.70 \times 10^{-4}$ and $K_{oc} = 254.6$. The values of K, K_{oc} were then discarded. A full PCE surrogate model was developed and the response surface interrogated to determine the values of K, K_{oc} that minimised the pointwise error between the PCE surrogate and the "Model" output. So for instance, the value $\mathrm{K} = 7.74 \times 10^{-4}$ minimised the percentage error at 0.52% for hydraulic conductivity and the value $K_{oc} = 254.2$ minimised the percentage error at 0.63% for organic carbon partition coefficient. Comparison with the error for other standard techniques can be found in the following table. Of interest is the number of model evaluations necessary to obtain this error.

Method	**Model Evals.**	**Predicted K**	**Predicted K_{oc}**
Brute Force	10201	7.60×10^{-4}	250.4
Interpolated Surface	121	7.84×10^{-4}	260.0
PCE Surface	121	7.74×10^{-4}	256.2
Conjugate Gradient	5683	7.75×10^{-4}	256.4
Conjugate Gradient	~500,000	7.70×10^{-4}	254.6

Table 2 Parameter finding using PCE compared to other standard techniques

The results for two different cases are visualized in Figure 7 where it can be seen that the error is indeed minimised in the vicinity of the correct point in the parameter space. It is seen that an "almost linear slice" of values through the parameter space results in good fits with the data, but with the best fits indeed occurring at the correct location in the parameter space. Minimisation of the error between data and model predictions thus does successfully find parameter values for this problem, even when a PCE surrogate is used instead of the full model to generate these model predictions.

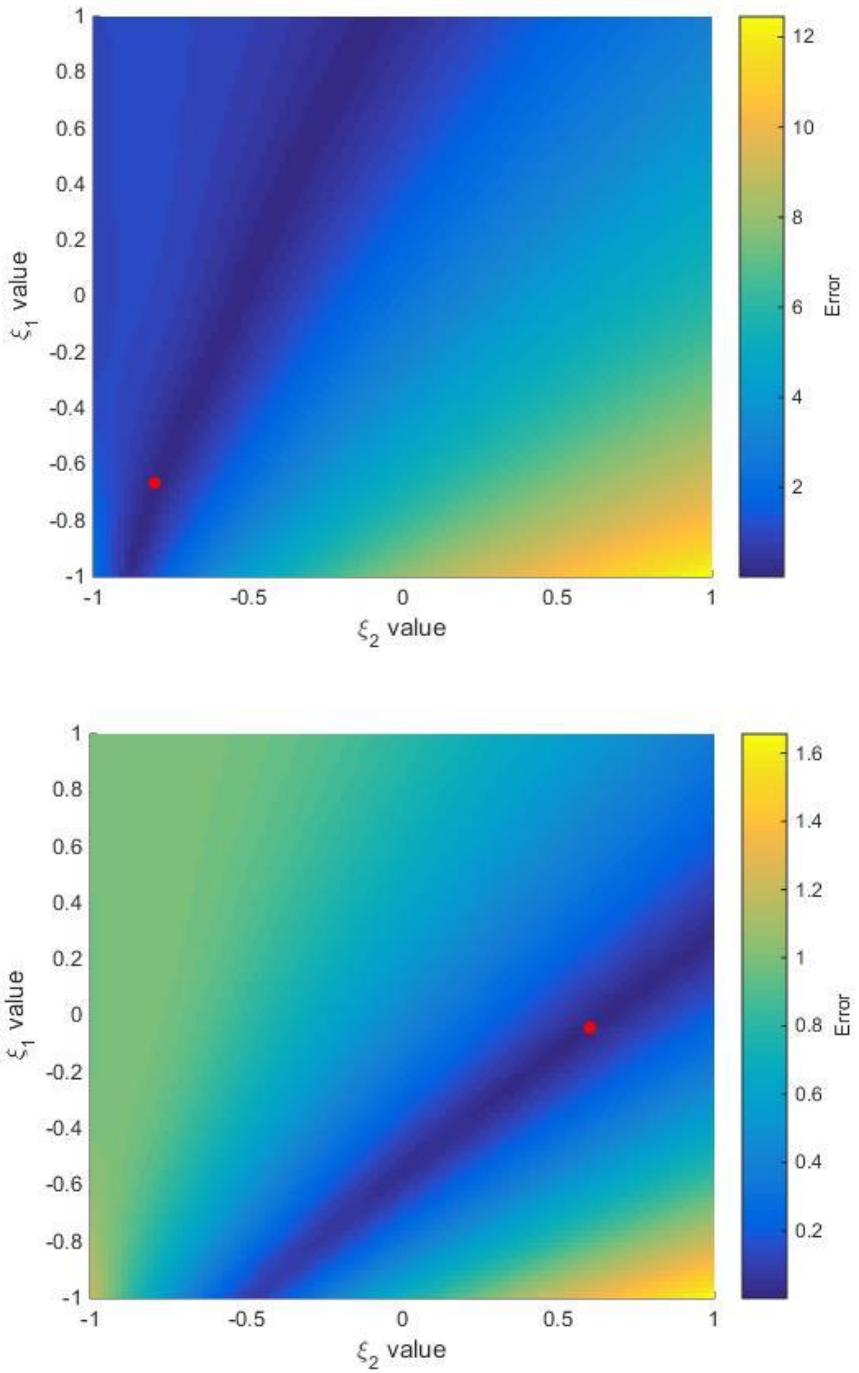

Figure 7 For the parameter space (hydraulic conductivity vs organic carbon partition coefficient) these error maps shows the (logarithmic) variation between the data generated directly from the underlying model and the solutions predicted by a PCE surrogate model with order *n=10*. The "true" parameter values used to generate the data are shown by the red dot.

Model 2. Surrogate to a 4-variable commercial Black-box model.

W1. The relevant "Model" to be approximated by PCE

Extraction of adsorbed gases:

The Computer Modelling Group's (CMG) `black box' solver for predicting the extraction of adsorbed gases was approximated using a non-intrusive PCE surrogate model. A model is built around a radial grid system referenced by *x*-, *y*- and *z*- axes which, respectively, are divided into 40 by 36 by 6 cells, as shown in Figure 8. The radial size is taken to be 600m and coal seam thickness is 5 m, which is about an average coal seam thickness in the Upper Juandah formation of the Surat Basin. One well is located at centre and perforated at all six layers. The top depth of this model is *440 m* which is similar to the average burial depth of Upper Juandah in the Surat Basin. The "Model's" properties are listed in Table 3. The initial pressure in cleats is *4440 kPa* at a reference depth of *440 m* by assuming a hydrostatical pressure system while the initial pressure in the matrix is assigned as *2750 kPa*. This leads to an initial gas saturation of about 77% in the matrix. A desorption time of 0.4 days is sourced from communications with an Australian CSG company.

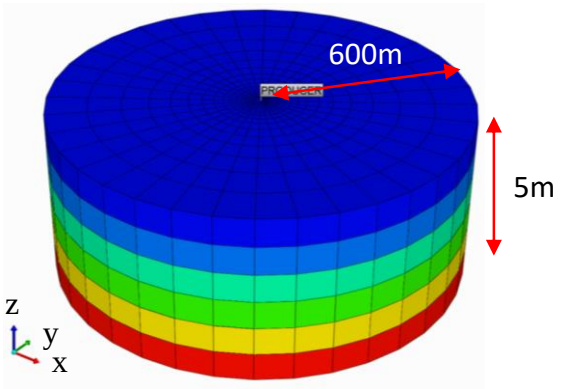

Figure 8 Grid system for numerical simulation.

Parameters	Ranges	Unit
Model	Dual porosity	-
Shape factor formulation	Gilman-Kazmi	-
Fluid component model	Peng-Robinson equation	-
Model geometry	Radial grid	-
Grid system	40×36×6	-
Thickness, h	5	m
Matrix porosity, ϕ_m	0.01	%
Fracture porosity, ϕ	[0.005,0.05]	%
Matrix permeability, k_m	0.01	mD
Fracture permeability in x-direction, k_x	[10,1000]	mD
Initial reservoir pressure in fracture, P_{rf}	4440	kPa
Initial reservoir pressure in matrix, P_{rf}	2750	kPa
Reservoir temperature, T_r	45	°C
Langmuir pressure, P_L	[0.00017,0.0003]	kPa
Langmuir volume, V_L	[0.2,1]	gmole/kg
Sorption time, τ	0.4	days
Coal density, ρ	1435	kg/m^3
Well bottom-hole pressure, BHP	300	kPa
Relative permeability, k_r	Corey equation with exponent of 2	
Separation condition	15°C and 101.3 kPa	

Table 3 Reservoir properties and ranges used in simulation.

W2. For "black box" model identify uncertain variables, their ranges and the associated probability distributions.

Four uncertain variables:

- Fracture permeability k_x, range $[10,1000]mD$
- Fracture porosity ϕ, range [0.005,0.05] %
- Langmuir volume V_L, range [0.2,1] gmole/kg
- Langmuir pressure P_L, range [0.00017,0.0003] kPa

A uniform distribution was assumed.

W3. Rescale the parameters to standard ranges.

$$\xi_1 = \frac{2(k_x - \overline{k_x})}{k_{x_{max}} - k_{x_{min}}} \qquad \xi_2 = \frac{2(\phi - \overline{\phi})}{\phi_{max} - \phi_{min}} \qquad \xi_3 = \frac{2(V_L - \overline{V_L})}{V_{L_{max}} - V_{L_{min}}} \qquad \xi_4 = \frac{2(P_L - \overline{P_L})}{P_{L_{max}} - P_{L_{min}}}$$

W4. The error tolerance was set 2%.

W5. The correct class of orthogonal polynomials is Legendre.

$$(m+1)L_{m-1}(\epsilon) = (2m+1)\varepsilon L_m(\varepsilon) - mL_{m-1}(\varepsilon)$$

$$L_1(\varepsilon) = \epsilon$$

$$L_0(\varepsilon) = 1$$

W6. A non-intrusive PCE surrogate model was developed.
W7. The initial order *n* of the PCE was set at *n=5*.
W8. Workflow for non-intrusive PCE was executed.

NI.1. For this model a non-intrusive PCE implementation was developed using both standard Gaussian quadrature and sparse grid quadrature, both are reported on here.
NI.2. Training (quadrature) points, associated weights and numerical integration code were generated. The number of training points are given below.

PCE Level	Number of training points	
	Gaussian quadrature	**Sparse grid quadrature**
n=5	1296	1105
n=6	2401	2929

Table 4 Number of training points

It is not possible to visualize the grids for levels *n=5* and *n=6* but to give an idea of the sparse grid distribution, grids for levels *n=2* and *n=3* are displayed in Figure 9.

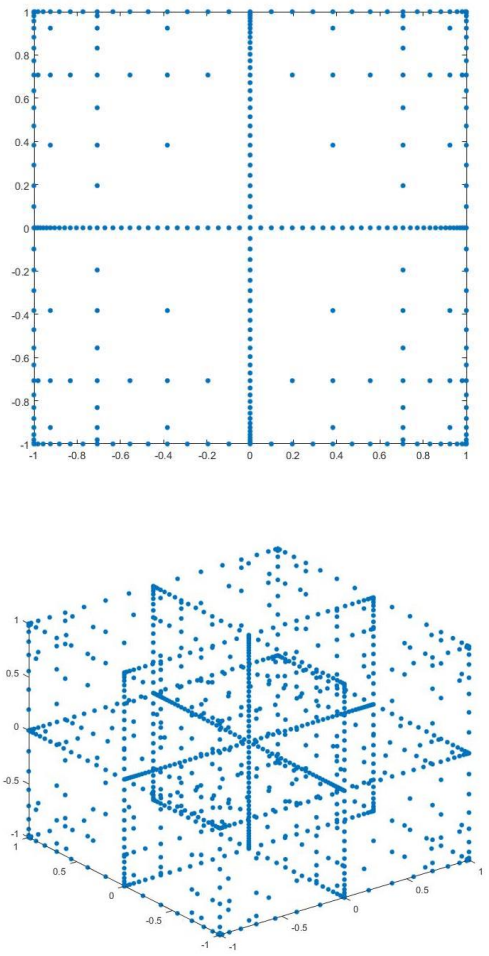

Figure 9 Sparse grids for n=2 and n=3.

NI.3. The "black box" model was evaluated at 1296 training points for Gaussian quadrature and 1105 training points for sparse grid quadrature and the Cumulative Gas and Peak Gas were calculated.

NI.4. The coefficients Y_k were determined using $Y_{\boldsymbol{k}} = \frac{\int_{\Omega} \mathrm{M}(\boldsymbol{\xi}) P_{\boldsymbol{k}}(\boldsymbol{\xi}) \rho(\boldsymbol{\xi})\, d\boldsymbol{\xi}}{\langle P_{\boldsymbol{k}}(\boldsymbol{\xi})^2 \rangle}$.

NI.5. A PCE surrogate model $Y \approx \sum_{k=0}^{n} Y_k P_k(\varepsilon_1, \cdots, \varepsilon_d)$ was determined.

W9. Execute calibration and validation procedures.

Calibration

C1.—C3. The order was initially set at *n=5* and incremented to *n=6* with the Y_k converging so *n=5* was within the given tolerance.

C4. The coefficients and the surrogate model were accepted.

Validation

V1.-V2. The point to point Root Mean Square error was calculated across the entire parameter space

$$RMS = \sqrt{\frac{E}{N}}$$

where *N* is the number of points and

$$E = \sum_{i=1}^{N} \left(S(x_i,\, t_i) - S_{PCE}(x_i,\, t_i) \right)^2.$$

The error for level *n=5* is shown in Table 5 and it can be seen that across both cumulative and peak gas the error was not within the given tolerance. Therefore the order of the PCE was increased to *n=6* giving the required tolerances.

Method	**Model Evals.**	**% error RMS**	
		Cumulative Gas	**Peak Gas**
Full grid PCE, p = 5	1296	2.54%	0.46%
Full grid PCE, p = 6	2401	1.67%	0.39%
Sparse PCE, p = 5	1105	2.68%	1.68%
Sparse PCE, p = 6	2929	1.72%	2.10%

Table 5 The percentage error for Cumulative and Peak Gas using the PCE surrogate model.

V4.-V7. The model was tested against a simulation based on latin hypercube sampling, using 3000 sample points and the error remained within the given tolerance.

W9. Statistical information.

The Cumulative Distribution Function (CDF) was calculated for both cumulative gas and peak gas with the results visualized in Figure 10.

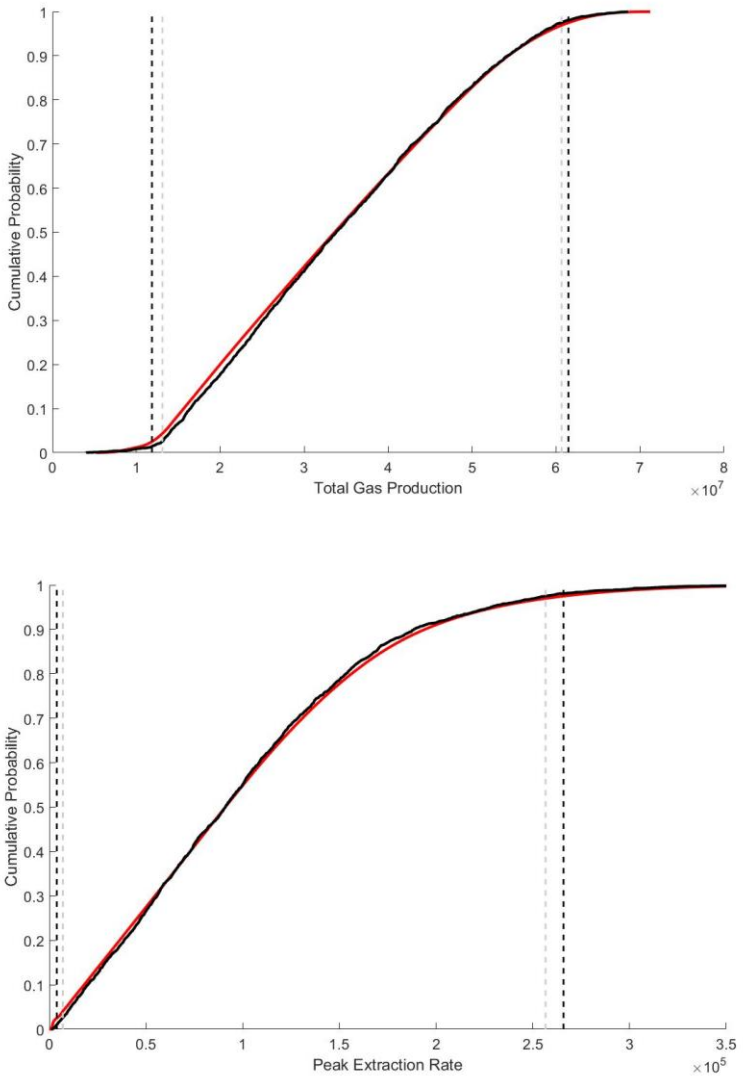

Figure 10 Confidence intervals and cumulative distribution functions for the total gas production and the peak extraction rate. The CDF for the PCE surrogate is the red line and the CDF for the simulation based on the 3000 latin hypercube sample points is in black.

The confidence intervals are large as the simulation was across the entire possible range of parameters and this would be reduced if the parameter ranges were refined.

Model 3. Surrogate to a 4-variable hexagonal grid cellular automata

Cellular Automata: Cellular automata are locally rule based models that can exhibit highly non-linear behaviour. The resulting data can show sharp fronts. We developed a cellular automata model to test the calibration and validation procedures of a surrogate PCE model. The sole purpose was to quantify the error in a surrogate PCE model for a highly non-linear system that exhibited volatile stochastic behaviour. For example, can a low order PCE produce good accuracy in such situations?

A cellular automata, based on a hexagonal grid with four uncertain variables, was approximated using a non-intrusive PCE surrogate.

We chose to use a well-known cellular automata model and used it to predict the spread of fire. The uncertain variables were taken to be initial fuel load, wind strength, base burn rate and burn variance with the output quantifying the total amount of burnt fuel, % variability across regions and maximum distance. Simulations were initiated by a change (fire ignition) in state for a central grid site, and at each time step a specified rule governed changes in the state of neighbouring sites. For each set of specific variable values, repeated simulations were executed until the mean output was within a given tolerance.

This is on-going work with the results not in a format to display here. However, a PCE of level *n=6* using standard grid training points, produced a surrogate model with errors within given tolerances.

5. Timing

The number of model evaluations to obtain the required tolerances has been given earlier. But for completeness these results are summarized in Table 6.

Method	Model Evaluations(% error RMS)		
	Model 1: 2 uncertain variables	Model 2: 4 uncertain variables	
		Cumulative Gas	Peak Gas
PCE Gaussian quad: Level 5	36(2.69×10^{-2})	1296(2.54×10^{-2})	1296(4.6×10^{-3})
PCE Sparse quad: Level 5	-	1105(2.68×10^{-2})	1105(1.68×10^{-3})
PCE Gaussian quad: Level 6	49(1.87×10^{-2})	2401(2.54×10^{-2})	2401(4.6×10^{-3})
PCE Sparse quad: Level 6	-	2929(1.72×10^{-2})	2929(2.01×10^{-3})
PCE Gaussian quad: Level 10	121(7.5×10^{-3})	-	-

Table 6 Number of training points and hence evaluations of the "Model" to obtain a PCE surrogate with the state error.

6. Conclusions

As demonstrated, the PCE surrogate approximates the two test models using a small number of evaluations and with a relatively small error.

PCE can be used to explore the parameter space, and given the relatively low computational cost it can easily be evaluated at a very large number of points in order to identify candidate parameter sets that could reproduce the observed data.

The difference in running time between PCE and other methods is pronounced. The performance of the method versus "traditional" exploration of the parameter space via a large number of full model evaluations has been summarized, with the PCE surrogate model demonstrating very good performance.

The PCE surrogate also provided direct access to statistical information such as Cumulative Distribution Function, Confidence Intervals, Mean and Variance.

7. Future Directions

- To work with industry partners to test PCE on industry data sets and simulated by standard commercial packages.
- Fully specify and optimise algorithms, with a focus on updating workflows for higher dimensional models.
- Refine calibration techniques and acceptance protocols.
- Investigate using local block-decompositions constructions with a view to combining local block statistics to obtain global statistics.
- Develop Petrel plug-in for PCE.
- Final Report and Presentation to Technical Working Group.

8. A Brief Review of the Theory

Uncertainty quantification in modelling processes is multifaceted including:

1. Estimation of uncertainty in model inputs
2. Propagation of uncertainty of inputs to model outputs
3. Estimation of uncertainty in model outputs.

Historically, Monte Carlo methods have been widely applied as a stochastic technique that uses randomness in the input variables to model uncertainty in the outputs. It involves repeated simulations based on pseudo-random inputs to generate a set of model outputs. However the required number of simulations to achieve acceptable error can be prohibitive. Thus the challenge is to develop efficient and effective techniques for harnessing this random process while still successfully capturing the uncertainty in the

input parameters.

Polynomial Chaos is a stochastic method that has recently been applied to quantify uncertainty in physical input parameters and an associated basis of polynomials to propagate this uncertainty to model outputs with a limited number of simulations.

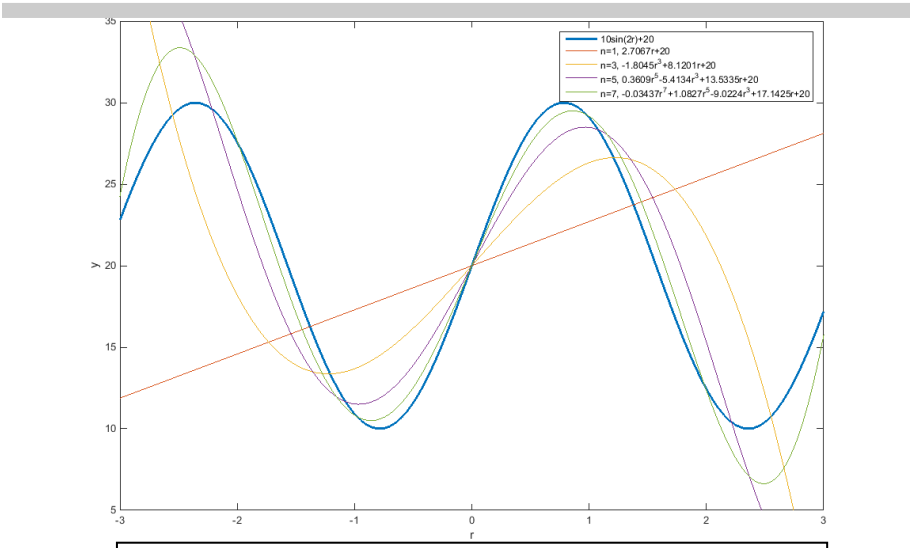

A plot of PCEs of varying degree using a Hermite Polynomial basis to approximate a periodic function.

Thus Polynomial Chaos, PC, allows for uncertainty quantification of input parameters and response outputs within a probabilistic framework. This framework allows for the physical characteristics, such as the topology and geometry of the region, or substance variation and impurities, to be incorporated into the system.

The central technique of Polynomial Chaos is the use of orthogonal polynomials as a basis for the fitting of response outputs based on a probabilistic data set. This data set may be the result of some experiment or simulation for which we want to fit a response surface, or alternatively the data may be instances of uncertain input values to variables within a model or simulation.

Principle Ideas

To explain the concept of PC we will restrict our discussion to a model with 2 input variables and 1 output variable so in 3- dimensional space. The inputs will be denoted *x* and *y* and the outputs *z=f(x,y).* It will be assumed that a number of sample points

$$(x_1, y_1), (x_2, y_2), \dots, (x_n, y_n)$$

are chosen as input to the model giving output values

$$z_1 = f(x_1, y_1),\ \ z_2 = f(x_2, y_2)\ \ , \dots, z_n = f(x_n, y_n)$$

The initial goal is to fit a response surface z=X(x,y)≈f(x,y) using these values z_1, z_2, …, z_n; that is, we wish to identify a suitable function X(x,y) that approximates the response distribution f(x,y) using PCE.

To explain the basic theory of PC we digress and give an analogy to aid understanding.

Take any point *X=(x,y,z)* in 3-dimensional space. This point can be written as

$$X = x[1,0,0] + y[0,1,0] + z[0,0,1], \qquad x, y, z \in \mathbb{R}.$$

That is, the point *X* can be written as a linear combination of the three basis vectors

$$[1,0,0], [0,1,0], [0,0,1].$$

In 3-dimensional space these three vectors are at right angles to each other and are said to be *orthogonal* to each other; that is,

$$[1,0,0].[0,1,0] = 1.0 + 0.1 + 0.0 = 0,$$

$$[1,0,0].[0,0,1] = 1.0 + 0.0 + 0.1 = 0,$$

$$[0,1,0].[0,0,1] = 0.0 + 1.0 + 0.1 = 0.$$

So, for instance, we can solve directly for *x* by using

$$x = X.[1,0,0].$$

This orthogonality property significantly reduces computation.

In general we want to find a function that can be used to approximate the surface passing through the sample points.

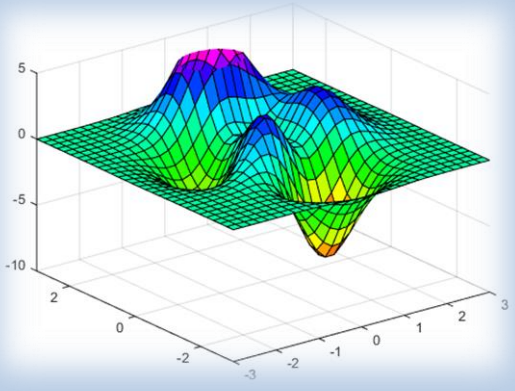

More precisely, based on this data we want to identify orthogonal polynomials $\phi_1, \phi_2, \dots, \phi_q$ and coefficients $w_1, w_2, \dots, w_q$ such that

$$X(x,y) = w_1\phi_1(x,y) + w_2\phi_2(x,y) + \cdots + w_q\phi_q(x,y) \approx f(x,y)$$

Here distinct polynomials ϕ_j and ϕ_k are *orthogonal* if the expected value of the product is zero; that is,

$$\mathbb{E}(\phi_j\, \phi_k) = \int \phi_j(\epsilon)\phi_k(\epsilon)p(\epsilon)d\epsilon = 0,$$

where p is the probability density function for the random variable ϵ. The theory tells us that the coefficients $w_1, w_2, \ldots, w_q$ can be evaluated as

$$w_k = \frac{\mathbb{E}(\phi_k\, f)}{\mathbb{E}(\phi_k\, \phi_k)} = \frac{\int \phi_k(\epsilon) f(\epsilon) p(\epsilon) d\epsilon}{\int \phi_k(\epsilon) \phi_k(\epsilon) p(\epsilon) d\epsilon},$$

where we choose the sample points (x_i, y_i) to be the quadrature points need to numerically compute $\int \phi_k(\epsilon) f(\epsilon) p(\epsilon) d\epsilon$. The orthogonal polynomials "play nicely together" and reduce the necessary computation.

In addition, we want the model to capture the uncertainty and variability in our parameters so we choose the underlying probability distribution and associated set of orthogonal polynomials accordingly. In particular, if the sample points are from a uniform distribution.

The mathematical theory behind Polynomial Chaos tells us such an approximation is possible and numerical quadrature allows us to achieve this with reduced costs.

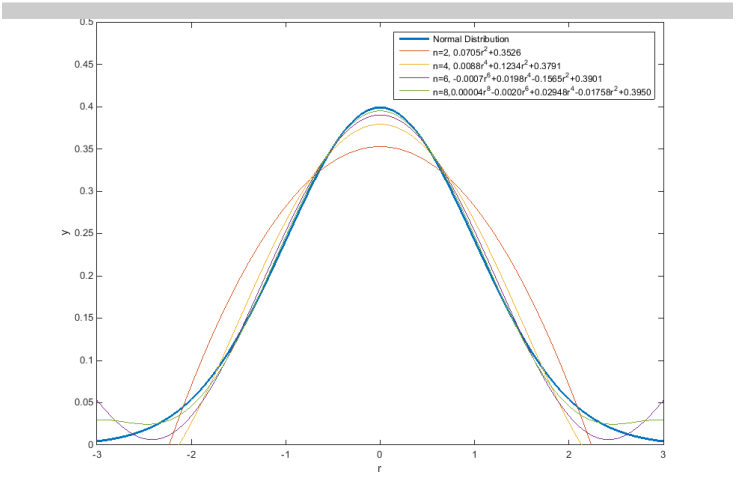

Higher degree PCEs approximate the underlying distribution more accurately.

Advantages and Disadvantages

Advantages of Polynomial Chaos:

- fast and efficient
- different probability distributions can be assigned to input parameters
- a spectral representation for the random process in terms of orthogonal basis functions, thus simplifying implementation
- relatively low degree polynomials usually give small error
- reduces computation cost significantly when compared to brute force methods such as Monte-Carlo simulations
- easy access to the statistics of the random outputs including moments and the cumulative distribution function, providing an expansion where the zero-index term contains the solution mean
- sensitivity to the chosen probability distribution and thus the variability in parameters and propagates this effect through the model to the response
- can use existing commercial solvers with non-intrusive Polynomial Chaos
- can accommodate a large number of uncertain parameters.

Disadvantages of Polynomial Chaos:

- Non-normal random input distributions must be treated with care. Generalised polynomial chaos and the Askey scheme are techniques suggested to increase rate of convergence [Choi et. al. (2004)] or transformation techniques [Tatang (1995)]
- convergence domains must be studied with care for both smooth and non-smooth outputs [Crestaux et.al. (2009)]
- PC does not quantify the approximation error as a component of uncertainty [O'Hagan (2013) p. 10]
- changing the input distribution could require the output strengths to be recomputed and also the convergence and truncation parameter to be recomputed [O'Hagan (2013) p. 15]
- Intrusive Polynomial Chaos requires modification of the solver. This is usually not feasible where commercial black box solvers are used. Moreover even if one has and can modify the source code the resulting solver may exhibit instability and, even if it doesn't, most likely will run extremely slowly.

9. Bibliography

References

[1] A. Alexanderian, O.P. Le Maître, H.N. Najm, M. Iskandarani, and O.M. Knio. Multiscale stochastic preconditionners in non-intrusive spectral projection. *J. Scientific Computing*, 50(7):306–340, 2012.

[2] M.J. Asher, B.F.W. Croke, and A.J. Jakeman. A review of surrogate models and their application to groundwater modeling. *Water Resources Research*, 521(8):5957–5973, 2015.

[3] Allison Ball, Shamim Ahmad, Kieran Bernie, Caitlin McCluskey, Pam Pham, Christian Tisdell, Thomas Willcock, and Alex Feng. Australian energy update 2015. Technical report, Office of the Chief Scientist, Australian Government, 2015. accessed on 1/6/2016.

[4] L.R. Bissonnette and S.A. Orszag. Dynamical properties of truncated Wiener-Hermite expansions. *Phys. Fluids*, 10(12):2603–2613, 1967.

[5] K. Burrage, P. Burrage, D. Donovan, and H.B. Thompson. Populations of Models, Experimental Designs and Coverage of Parameter Space by Latin Hypercube and Orthogonal Sampling. *Procedia Computer Science*, 51:1762–1771, 2015.

[6] K. Burrage, P.M. Burrage, D. Donovan, T. McCourt, and H.B. Thompson. Estimates on the coverage of parameter space using populations of model. In *Modelling and Simulation, IASTED, ACTA Press*, 2014.

[7] R.H. Cameron and W.T. Martin. The orthogonal development of nonlinear functionals in series of fourier-hermite functionals. *Ann. Math.*, 48(2):385–392, 1947.

[8] Seung-Kyum Choi, Ramana V Grandhi, Robert A. Canfield, and Chris L. Pettit. Polynomial chaos expansion with latin hypecube sampling for estimating response variability. *AIAA Journal*, 42(6):1191–1198, 2004.

[9] S.K. Choi, R. V. Grandhi, and R. A. Canfield. Structural reliability: non-gaussian stochastic behaviour. *Computers and Structures*, 82(13,14):1113–1121, 2004.

[10] A.J. Chorin. Gaussian fields and random flow. *J. Fluid Mech.*, 85:325–347, 1974.

[11] S Cremaschi, G.E. Kouba, and Subramani H.J. Characterization of confidence in multiphase flow predictions. *Energy and Fuels*, 26(7):4034–4045, 2012.

[12] T. Crestaux, O. Le Maître, and J.-M. Martinez. Polynomial chaos expansion for sensitivity analysis. *Reliability Engineering and System Safety*, 94(7):1161–1172, 2009.

[13] S.C. Crow and G.H. Canavan. Relationship between a Wiener-Hermite and an energy cascade. *J. Fluid Mech.*, 41(2):387–403, 1970.

[14] D. Datta and Kushwaha.S. Uncertainty quantification using stochastic response surface method case study-transport of chemical contaminants through groundwater. *International Journal of Energy, Information and Communication*, 2(3):49–58, 2011.

[15] B. Debusschere, H. Najm, Sargsyan K., and Safta C. Polynomial chaos based uncertainty propogation intrusive and non-intrusive methods. Published at http://venus.usc.edu/UQ-SummerSchool-2012/Debusschere.pdf, 2012.

[16] B. Debusschere, H. Najm, A. Matta, O. Knio, R. Ghanem, and O. Le Maître. Protein labeling reactions in electrochemical microchannel flow: Numerical simulation and uncertainty propagation. *Physics of Fluids*, 15(8):2238–2250, 2003.

[17] Bert Debusschere. Lecture 1: Uncertainty and spectral expansions. In Ghanem [23].

[18] Bert Debusschere. Lecture 2: Forward propagation: Intrusive and non-intrusive. In Ghanem [23].

[19] Bert J. Debusschere, Habib N. Najm, Philippe P. Pebay, Omar M. Knio, Roger G. Ghanem, and Olivier P. Le Maître. Numerical challenges in the use of polynomial chaos representations for stochastic processes. *SIAM J. Sci. Comput.*, 26:698–719, 2004.

[20] F. Dottori and E. Todini. Developments of a flood inundation model based on cellular automata: Testing different methods to imporve model performance. *Physics and Chemistry of the Earth*, 36:266–280, 2011.

[21] J. A. M. S. Duarte, Muhammad Sahimi, and João Marques de Carvalho. Dynanmic permeability of porous media by cellular automata. *Journal de Physique II*, 2(1):1–5, Jan 1992.

[22] R. Ghanem and Dham S. Stochastic finite element analysis for multiphase flow in heterogeneous porous media. *Transport in Porous Media*, 32:329–262, 1998.

[23] Roger Ghanem, editor. *Polynomial Chaos Based Uncertainty Propagation*. US Department of Energy (DOE), Office of Advanced Scientific Computing Research (ASCR), Scientific Discovery through Advanced Computing (SciDAC) and Applied Mathematics Research (AMR) programs., 2013.

[24] Roger G. Ghanem and Pol D. Spanos. *Stochastic Finte Elements: A Spectral Approach*. Springer-Verlag, 1991.

[25] L. Gilli, D. Lathouwers, J. L. Kloosterman, T. H. J. J. van der Hagen, A. J. Koning, and D. Rochman. Uncertainty quantification for criticality problems using non-intrusive and adaptive polynomial chaos techniques. *Annals of Nuclear Energy*, 56:71–80, 2013.

[26] Recep M. Gorguluarslan, Sang-In Park, David W. Rosen, and Seung-Kyum Choi. Material characterization of additively manufactured part via multi-level stochastic upscaling method. *Proceedings of the ASME 2015 International Design Engineering Technical Conferences & Computers and Information in Engineering Conference*, August 2-5, 2015, Boston, Massachusetts, USA:DETC2015–46822, 2015.

[27] Ihsan Hamawand, Talal Yusaf, and Sara G. Hamawand. Coal seam gas and associated water: A review paper. *Renewable and Sustainable Energy Reviews*, 22:50–560, 2013.

[28] F. Hossain, E.N. Anagnostou, and K.-H. Lee. A non-linear and stochastic response surface method for bayesian estimation of uncertainty in soil moisture simulation from a land surface model. *Nonlinear Processes in Geophysics*, 11:427–440, 2004.

[29] S. Hurter, N. Marmin, P. Probst, and A. Garnett. Probabilistic estimates of injectivity and capacity for large scale CO_2 storage in the gippsland basin victoria australia. *Energy Procedia*, 37:3602–3609, 2013.

[30] Jan-Dirk Jansen, Okko H. Bosgra, and Paul M.J. Van den Hof. Model-based control of multiphase flow in subsurface oil reservoirs. *Journal of Process Control*, 18:846–855, 2008.

[31] J.D. Jansen, S.D. Douma, D.R. Brouwer, P.M.J. Van den Hof, O.H. Bosgra, and A.W. Heemink. Closed-loop reservoir management. *SPE International*, SPE 119098, 2009.

[32] Lemont B. Kier, Chao-Kun Cheng, and Bernard Testa. A cellular automata model of the percolation process. *J. Inf. Comput. Sci.*, 39:326–332, 1999.

[33] A. Koponen, M. Kataja, and J. Timonen. Permeability and effective porosity of porous media. *Physical Review E*, 56:3319–3325, 1997.

[34] A.C.J. Korte and H.J.H. Brouwers. cellular automata approach to chemnical reactions; 1 reaction controlled systems. *Chemical Engineering Journal*, 228:172–178, 2013.

[35] Eric Laloy, Bart Rogers, Jasper Vrugt, Dirk Mallants, and Diederick Jacques. Efficient posterior exploration of a high-dimensional groundwater model for two stage markov chain mpnte carlo simulation and polynomial chaos expansion. *Water Resoruces Research*, 49:2664–2682, 2013.

[36] Brodie A. J. Lawson, Bevan Thompson, Stephen Tyson, and Diane Donovan. Non-intrusive Polynomial Chaos for the Approximation of Hydrological Parameters. *submitted*, 2016.

[37] O.P. Le Maître, M.T. Reagan, H. Najm, R. Ghanem, and O.M. Knio. A stochastic projection method for fluid flow: Ii. random process. *Journal of Computational Physics*, 181:9–44, 2002.

[38] S.H. Lee and W. Chen. A comparitive study of uncertainty propogation method for black-box-type problems. *Struct Multidisc Optim*, 37:239–253, 2009.

[39] H. Li and D. Zhang. Probabilistic collocation method for flow in porous media: Comparisons with other stochastic methods. *Water Resources Research*, 43:1–13, 2007.

[40] H. Li and D. Zhang. Efficient and accurate quantification of uncertainty for multimulti flow with the probabilistic collocation method. *Society of Petroleum Engineers*, 14(4):665–679, 2009.

[41] Heng Li, Pallav Sarma, and Dongxiao Zhang. A comparative study of the probabilistic-collocation and experimental design methods for petroleum-reservoir uncertainty quantification. *SPE Journal*, 16(2):429–439, 2011.

[42] D Lucor and M S Triantafyllou. Parametric study of a two degree-of-freedom cylinder subject to vortex-induced vibrations. *Journal of Fluids and Structures*, 24(8):1284–1293, 2008.

[43] L. Mathelin and M.Y.and Zang T.A. Hussaini. Stochastic approaches to uncertainty quantification in cfd simulations. *Numerical Algorithms*, 38(1-3):209–236, 2005.

[44] L. Mathelin and O.P. Le Maître. Uncertainty quantification in a chemical system using error estimate-based mesh adaptation. *Theoretical and Computational Fluid Dynamics*, 28(5):415–434, 2012.

[45] M.D. McKay. Latin Hypercube sampling as a tool in uncertainty analysis of computer models. In J.J. Swain, D. Goldsman, R.C. Crain, and J.R. Wilson, editors, *Proceedings of the 1992 Winter Simulation Conference*, pages 557–564, 1992.

[46] M.D. McKay, Beckman, and Conover W.J. A comparison of three methods for selecting values of input variables in the analysis of output for a computer code. *Technometrics*, 21:239–245, 1979.

[47] W.C. Meecham and D.T. Jeng. Use of the Wiener-Hermite expansion for nearly normal turbulence. *J. Fluid Mech.*, 32:225–249, 1968.

[48] W.C. Meecham and A. Siegel. Wiener-Hermite expansion in model turbulence at large reynolds numbers. *Phys. Fluids*, 7:1178–1190, 1964.

[49] Peter Müller. Lectures 5-6: Nonparametric bayesian inference. In Ghanem [23].

[50] H. Najm. Uncertainty quantification and polynomial chaos techniques in computational fluid dynamics. *Annual Review of Fluid Mechanics*, 41:35–52, 2009.

[51] Erich Novak and Klaus Ritter. Simple Cubature Formulas with High Polynomial Exactness. *Constructive Approximation*, 15:499–522, 1999.

[52] Anthony O'Hagan. Polynomial chaos: A tutorial and critique from a statistician's perspective. Submitted to SIAM/ASA Journal of Uncertainty Quantification, 2013.

[53] S. Oladyshkin and W. Nowak. Data-driven uncertainty quantification using the arbitrary polynomial chaos expansion. *Reliability Engineering and System Safety*, 106:179–190, 2012.

[54] M. Paffrath and U. Wever. Adapted polynomial chaos expansion for failure detection. *Journal of Computational Physics*, 226:263–281, 2007.

[55] Zhejun Pan and Luke D. Connell. Modelling permeability for coal reservoirs: a review of analytical models and testing data. *International Journal of Coal Geology*, 92:1–44, 2012.

[56] Ernesto Esteves Prudencio. Lectures 3-4: The use of Bayes formula in calibration, ranking, averaging, filtering, optimal design of experiments, and emulation with gaussian processes. In Ghanem [23].

[57] S. Psaltis, T.W. Farrell, K. Burrage, P. Burrage, P. McCabe, T.J. Moroney, I. Turner, and S. Mazumder. Mathematical modelling of gas production and compositional shift of a csg field 1: Local model development. *Energy*, 2015.

[58] G. Ravazzani, D. Rametta, and M. Mancini. Macroscopic cellular automata for groundwater modelling: A first approach. *Environmental Modelling and Software*, 26:634–643, 2011.

[59] M.T. Reagan, H.N. Najm, R.G. Ghanem, and O.M. Knio. Uncertainty quantification in reaction flow simulations through non-intrusive spectral projection. *Combustion and Flame*, 132:545–555, 2003.

[60] M. Rousseau, O. Cerdan, A. Ern, O. Le Maître, and P. Sochala. Study of overland flow with uncertain infiltration using stochastic tools. *Advances in Water Resources*, 38:1–12, 2012.

[61] Carl Philip Rupert and Cass T. Miller. An analysis of polynomial chaos approximations for modeling single-fluid-phase flow in porous medium systems. *Journal of Computational Physics*, 226(2):2175–2205, 2007.

[62] P. Sarma, L.J. Durlofsky, and K. Aziz. Efficient closed-loop production optimisation under uncertainty. *Society of Petroleum Engineersprocess*, SPE 94241, 2005.

[63] P. Sarma and J. Xie. Efficient and robust uncertainty quantification in reservoir simulation with polynomial chaos expansions and non-intrusive spectral projection. *SPE International*, SPE 1411963, 2011.

[64] Fei Sha. Lectures 7-8: Kernels and Dimension Reduction. In Ghanem [23].

[65] A. Siegel, T. Imamura, and W.C. Meecham. Wiener-Hermite expansion in model turbulence in the late decay stage. *J. Math. Phys.*, 6:707–721, 1965.

[66] M. Stein. Large sample properties of simulations using Latin Hypercube sampling. *Technometrics*, 29(2):143–151, 1987.

[67] B. Sudret. Global sensitivity analysis using polynomial chaos expansion. *Reliability Engineering and System Safety*, 93:964–979, 2008.

[68] B. Sudret and A. Der Kiureghian. Stochastic finite element methods and reliability: A state of the art report. Technical Report UBC/SEMM-2000/08, University of California, Berkerley, November 2000.

[69] Klaus Sutner. Automata, a Hybrid System for Computational Automata Theory. In *Proceedings of the 7th Conference on Implementation and Application of Automata, LNCS 2608*, pages 221–227, Berlin, 2003. Springer-Verlag.

[70] Klaus Sutner. Cellular automata and percolation. Lecture notes 15-110: Principles of computing spring 2011, Carnegie Melon University, 2011.

[71] B. Tang. Orthogonal Array-Based Latin Hypercubes. *Orthogonal Array-Based Latin Hypercubes*, 88(424):1392–1397, 1993.

[72] M. A. Tatang. *Direct incorporation of uncertainty in chemical and environmental engineering systems*. PhD thesis, Mass. Inst. of Tech., 1995.

[73] Menner A . Tatang, Wenwei Pan, Ronald G. Prinn, and Gregory J. McRae. An efficient method for parametric uncertainty analysis of numerical geophysical models. *Journal Of Geophysical Research*, 102(D18):21925–21932, 1997.

[74] E. Tixier, D. Lombardi, B. Rodriguez, and J.F. Gerbeau. Variability modelling in cardiac epectrophysiology through an inverse uncertainty qantification approach. In P. Nithiarasu and E. Budyn, editors, *4th International Conference on Computational and Mathematical Biomedical Engineering - CMBE2015*, 2015.

[75] J. Tryoen, O. Le Maître, and A. Ern. Adaptive anisotropic spectral stochastic methods for uncertain scalar conservation laws. *SIAM J. Sci. Comp.*, 34(5):2459–2481, 2012.

[76] J.K. Vaurio. Uncertainties and quantification of common cause failure rates and probabilities for system analyses. *Reliability Engineering and System Safety*, 90:186–195, 2005.

[77] W.J. Welch, R.J. Buck, J. Sacks, H.P. Wynn, T.J. Mitchell, and M.D. Morris. Screening, Predicting, and Computer Experiments. *Technometrics*, 34:15–25, 1992.

[78] N. Wiener. The homogeneous chaos. *American Journal of Mathematics*, 60(4):897–936, 1938.

[79] D. Xiu and G.E. Karniadakis. Modeling uncertainty in flow simulations via generalized polynomial chaos. *Journal of Computational Physics*, 187:137–167, 2003.

[80] D Xiu, D. Lucor, C. H. Su, and G. E. Karniadakis. Stochastic modeling of flow-structure interactions using generalized polynomial chaos. *Journal of Fluids Engineering*, 124(1):51–59, 2002.

[81] D. Xiu and S.J. Sherwinb. Parametric uncertainty analysis of pulse wave propagation in a model of a human arterial network. *Journal of Computational Physics*, 226(2):1385–1407, 2007.

[82] B. Yeten, A. Castellini, B. Guyaguler, and Chen W.H. A Comparison Study on Experimental Design and Response Surface Methodologies. *SPE International*, SPE 93347, 2005.

[83] Y.K. Zhang. *Stochastic Methods for Flow in Porous Media Coping with Uncertainties*. Academic Press, 2001.